2mq

NASA CR-132894

A CONTRIBUTION TO THE SYNOPTIC CLIMATOLOGY OF THE EXTRATROPICS

BY

SRINIVASAN SRIVATSANGAM

Atmospheric Science
PAPER NO.
203

DEPARTMENT OF ATMOSPHERIC SCIENCE COLORADO STATE UNIVERSITY FORT COLLINS, COLORADO

$\mathcal{I}$

BIBLIOGRAPHIC DATA SHEET	1. Report No. CSU-ATSP-203	2.	3. Recipient's Accession No.

4. Title and Subtitle A Contribution to the Synoptic Climatology of the Extratropics	5. Report Date July, 1973
	6.

7. Author(s) SRINIVASAN SRIVATSANGAM	8. Performing Organization Rept. No. 203

9. Performing Organization Name and Address Dept. of Atmospheric Science, Coloardo State University Fort Collins, Colo. 80521	10. Project/XXXX/XXXX/XXXX No. 1989
	11. Contract/Grant No. NGR-06-002-098

12. Sponsoring Organization Name and Address National Aeronautics and Space Administration Washington, D. C.	13. Type of Report & Period Covered
	14.

15. Supplementary Notes

16. Abstracts
Relative geostrophic vorticity ζ_g is analyzed in terms of arithmetic and root mean square (r.m.s.) averaging. The latter averaging is appropriate for the middle latitudes. Analyses for January 1970 reveal the organization of the meanders of the Extratropical Frontal Jet Streams and the extension of baroclinicity from the jet-stream level to the surface.

17. Key Words and Document Analysis.   17a. Descriptors
    Synoptic Climatology
    Extratropics

17b. Identifiers/Open-Ended Terms

17c. COSATI Field/Group

18. Availability Statement Release Unlimited	19. Security Class (This Report) UNCLASSIFIED	21. No. of Pages 43 35
	20. Security Class (This Page) UNCLASSIFIED	22. Price 4.00

FORM NTIS-35 (REV. 3-72)   THIS FORM MAY BE REPRODUCED   USCOMM-DC 14952-P72

II

A CONTRIBUTION TO THE SYNOPTIC CLIMATOLOGY

OF THE EXTRATROPICS

by

Srinivasan Srivatsangam

Department of Atmospheric Science

Colorado State University

Fort Collins, Colorado

August, 1973

Atmospheric Science Paper No. 203

Abstract

A relationship is established between relative geostrophic
vorticity on an isobaric surface and the Laplacian of the underlying
layer-mean temperature. This relationship is used to investigate the
distribution of vorticity and baroclinicity in a jet-stream model which
is constantly recurrent in the winter troposphere. The investigation
shows that the baroclinic and vorticity fields of the extratropical
troposphere must be bifurcated with two extrema in the middle and
subpolar latitudes. This pattern is present in daily tropospheric
meridional cross-sections. The reasons for the disappearance of bifurcation
in the time-and-longitude averaged distributions are discussed.

The time-averaged zonal root mean square vorticity, called K for
brevity, is shown to be a parameter which overcomes this deficiency in
the presentation of meridional cross-sections of the atmosphere.

The meridional cross-sections of K indeed indicate that the upper
tropospheric vorticity--and by inference the tropospheric-mean baro-
clinicity--distribution is bifurcated in winter with one maximum over
30 - 45 N, another over 60 - 70 N and a relative minimum at 55 N.

The geographical distribution of the temporal r.m.s. vorticity shows
that the maximum of K over 30 - 45 N in the meridional cross-section
is due to three waves in the vorticity field at these latitudes. Two
of the three maxima imbedded in these waves occur over the
eastern coastlines of Asia and North America, and are considerably more
intense than the maximum occurring over Southern Asia. All three
maxima are quasi-zonally distributed. The maxima over the oceans
have their major axes in the vicinity of cold and warm ocean current
confluences. These maxima, moreover, do not protrude far into the continents.

i

The implications of the above geographical distribution for the maintenance of the observed kinetic energy and baroclinicity distributions in the extratropical troposphere in winter are discussed.

Lastly, it is shown that the subtropical and subpolar ridges are nearly antiparallely distributed as is required by the observed distribution of temporal r.m.s. vorticity at the jet-stream level.

A Note on Nomenclature

We shall denote by the term Extratropical Frontal Jet Streams (EFJ)
all jet streams which occur in the upper troposphere in conjunction with
lower tropospheric baroclinic zones or fronts. The subpolar (60-70 N)
branch of this jet stream will be called the Arctic Front Jet Stream (AFJ)
(see Reiter, 1963, p. 221-224; Petterssen, 1956, p. 208). The midlatitude
(35 - 50 N) branch of the same will be called the Polar Front Jet Stream
(PFJ).

We shall use the term "mean" to denote arithmetic mean only.
Wherever root mean square values are alluded to, the adjective "r.m.s."
will be used. The term "averaging" will be used to refer to both
arithmetic averaging and the process of obtaining r.m.s. values.

Relative geostrophic vorticity will be generally referred to as
vorticity.

TABLE OF CONTENTS

LIST OF TABLES

vi

1. Introduction

One apparent contradiction in meteorology is made obvious by a consideration of the winter mean meridional distribution of $[\bar{u}]$, i.e., the time-and-longitude averaged zonal wind component, and the mean meridional circulation in the same season (see, for example, Oort and Rasmusson, 1971, p. 23, 24 and 234). The $[\bar{u}]$ field has a maximum at about 30 N, 200 mb and decreases in all directions from that point. This represents, under the assumption of geostrophic flow, a maximum horizontal concentration of isotherms in the troposphere at 30 N and the presence of a hemispheric Hadley cell with warm air rising in the equatorial regions and cold air sinking in the polar regions, with a generation of kinetic energy in the region occupied by this cell, for otherwise friction will destroy the $[\bar{u}]$ field. But the mean meridional circulation shows an indirect cell in the middle latitudes which destroys zonal kinetic energy in the region occupied by that cell. These two illustrations are reconciled by partitioning the daily K.E. and available potential energy (A) fields into zonal-mean and eddy components. A study of these indicates the energy cycle of the atmosphere to be as in Fig. 1, which could be used to reconcile the mean meridional circulation and the field of $[\bar{u}]$ (see, for example, Lorenz, 1967, p. 97 - 113). Although our understanding of the atmospheric energy cycle is thereby enhanced, the meridional distributions remain poor representatives of the extratropical eddy field. However, the eddies are of considerable importance. Therefore we feel that there is a need for the proper meridional representation of extratropical eddies in time-mean cross-sections.

Table 1

Definitions of Symbols

A	Available potential energy
$\mathbb{B}$	The baroclinicity vector
$f(x,..), f(x,y,..)$ etc,	Mathematical functions; not the Coriolis parameter
f	$2\,\Omega \sin \phi$, the Coriolis parameter
H	Geopotential hgt
$K = [\{\zeta_g\}_{(\lambda)}]_{(t)} \simeq [\{\zeta_g\}_{(t)}]_{(\lambda)}$,	The time mean of the zonal root mean square vorticity
K.E.	Kinetic Energy
R	The gas constant for dry air
p	Pressure
t	Time
T	Temperature
u_g, v_g	Zonal and meridional components, respectively, of the geostrophic wind
β	$\partial f/\partial y$, the Rossby parameter
ζ_g	Relative geostrophic vorticity
λ	Longitude
ϕ	Latitude
$[f]_{(x)}$	The arithmetic mean of $f(x,...)$ in x
$[[f]_{(x)}]_{(y)} = [f]_{(x,y)}$	
$(f)_{(x)} = f(x,...) - [f]_{(x)}$	
$\{f\}_{(x)}$	Root mean square value of $f(x,...)$ in x
$([H]_{(\lambda)})_{(\phi)} = [H]_{(\lambda)} - [H]_{(\lambda,\phi)}$	The deviation of zonally averaged geopotential height of an isobaric surface from the hemispheric average in the present case

α — Symbol for proportionality

$|x|$ — Modulus of x

$<f(x,y)>$ — Matrix of f in x and y

$-$ — Layer-mean

$$\nabla_2^2 = (\frac{\partial^2}{\partial x^2} + \frac{\partial^2}{\partial y^2})$$ — The horizontal Laplacian operator

In the symbol $[\overline{u}]$ — $\overline{}$ is time average and [ ] is zonal average

Most of the existing parameters are poor representatives of the eddies (in time-and-zonal average distributions). One exception is perhaps the generation of kinetic energy. This parameter has been described well by Kung (1971), but there are many difficulties in estimating this parameter, especially over the data-sparse regions of the atmosphere.

Since, in general, vorticity is estimated more accurately than divergence on account of the magnitudes involved, we shall use geostrophic relative vorticity here to represent the eddies in time-and-zonal mean cross-sections.

We shall start by establishing a relationship between geostrophic relative vorticity over an isobaric surface and the Laplacian of the layer-mean temperature $\overline{T}$ of the underlying atmospheric layer. This relationship will enable a study of the association between vorticity and baroclinicity distributions in synoptic-scale extratropical eddies purely in terms of layer-mean temperatures.

2. A Relationship between the Thermal and Vorticity Fields

The zonal component of the geostrophic wind at pressure p_0 might be written as

$$u_{g,p_0} = u_{g,oo} - \frac{\partial u_g}{\partial p} |\delta p| \tag{1}$$

where $u_{g,oo}$ is the zonal component of the geostrophic wind at some higher pressure $p_0 + \delta p$. Substituting the geostrophic thermal wind in the x, y, p coordinate system, viz.,

$$\frac{\partial u_g}{\partial p} = \frac{R}{\bar{p} f} \frac{\partial \bar{T}}{\partial y} \tag{2}$$

(where the bar represents mean conditions in the layer p_0 to $(p_0 + \delta p)$ in equation (1) and differentiating with respect to y

$$\frac{-\partial u_{g,p_0}}{\partial y} = \frac{-\partial u_{g,oo}}{\partial y} + \frac{R}{\bar{p} f} \frac{\partial^2 \bar{T}}{\partial y^2} |\delta p| - \frac{R}{\bar{p}} \frac{\partial \bar{T}}{\partial y} \frac{\beta}{f^2} |\delta p| \tag{3}$$

The assumption that $\frac{\partial u_{g,oo}}{\partial y} \doteq 0$ is generally valid if $p_0 < 500$ mb and $(p_0 + \delta p) > 900$ mb.

If $\left(-\frac{\partial \bar{T}}{\partial y}\right)$ has a value of 0.16×10^{-6} $^{\circ}$K cm^{-1} in the baroclinic region and a value of 0.04×10^{-6} $^{\circ}$K cm^{-1} in the relatively barotropic air masses (see Fig. 3),

$$\frac{\partial^2 \bar{T}}{\partial y^2} \doteq -0.12 \times 10^{-14} \text{ }^{\circ}\text{K cm}^{-2}$$

if the changes in temperature gradients are obtained over 10 deg. latitude. These values are representative of middle latitude frontal systems. So, if the latitude is 45 deg. such that $f = 1.0 \times 10^{-4}$ s^{-1} and $\beta = 1.6 \times 10^{-13}$ cm^{-1} s^{-1}

$$\frac{-\dfrac{R}{\overline{p}}\dfrac{\partial \overline{T}}{\partial y}\dfrac{\beta}{f^2}|\delta p|}{\dfrac{R}{f\overline{p}}\dfrac{\partial^2 \overline{T}}{\partial y^2}|\delta p|} = \frac{0.16 \times 10^{-15}}{0.12 \times 10^{-14}}$$

$$\simeq 1 \times 10^{-1}$$

Hence the third term on the right hand side of equation (3) can be neglected in comparison with the second term. Thus

$$- \frac{\partial u_{g,p_0}}{\partial y} = \frac{R}{\overline{p}f}\frac{\partial^2 \overline{T}}{\partial y^2}|\delta p| \tag{4}$$

A similar equation is readily derived for $\dfrac{\partial v_g}{\partial x}$. The addition of the two equations then shows that

$$\zeta_{g,p_0} = \frac{R}{\overline{p}f}\left(\frac{\partial^2 \overline{T}}{\partial x^2} + \frac{\partial^2 \overline{T}}{\partial y^2}\right)|\delta p| \tag{5}$$

or,

$$\zeta_g \alpha \nabla_2^2 \overline{T} \tag{6}$$

This is the relationship that we sought.

3. Application to a Jet-Stream Model

We shall use this in the model of jet-stream flow illustrated in

Figure 2, which was inspired by a model presented earlier by Reiter (1972,

p. 69). Here the surface wind has been assumed to be zero everywhere

and hence the streamlines at the jet-stream level are parallel to

the tropospheric mean isotherms. In Fig. 3, the meridional temperature

gradient associated with the model of Fig. 2 is presented and in Fig. 4

the corresponding distribution of $\nabla_2^2 \overline{T}$. (N.B.: Here and hereafter

we shall refer to the layer-mean temperatures as temperatures).

From these illustrations it is seen that the vorticity maximum

is located slightly poleward of the region of maximum baroclinicity and

the vorticity minimum equatorward of the region of maximum baroclinicity

in that meridional sector. We use the term baroclinicity here to refer to

$\partial \overline{T}/\partial y$. However, an analysis of the field of the magnitude of the baro-

clinicity vector, i.e.,

$$ |B| = \left[\left(\frac{\partial \overline{T}}{\partial x} \right)^2 + \left(\frac{\partial \overline{T}}{\partial y} \right)^2 \right]^{\frac{1}{2}} $$

shows that the distribution of this quantity is not very different from

that of $\partial \overline{T}/\partial y$ except over the 50 - 70 longitude sector.

In Fig. 5 and 6 the zonal averages of $|B|$, $\frac{\partial \overline{T}}{\partial y}$, $\nabla_2^2 \overline{T}$ and the

zonal root mean square (r.m.s.) values of $\nabla_2^2 \overline{T}$ are presented. From

these averages it is seen that if the model of Fig. 2 is indeed representa-

tive of extratropical eddy flow, the zonal averages of the various

parameters considered here must be bifurcated with extrema in middle

and subpolar latitudes.

Figure 7 is the geopotential height field of the 300 mb surface for

Jan. 1, 1970. It is typical of the 300 mb height field on almost any day

in January 1970. From this illustration it is obvious that the model of Fig. 2 indeed occurs in daily maps.

At this point we shall digress from this discussion and elucidate our averaging conventions.

4. Averaging Conventions*

Here we shall follow the averaging conventions introduced by Reiter (1969a; 1969b, p. 6 - 8). The symbolism is defined in Table 1. A new extension of these conventions is introduced here. This is for the process of obtaining the r.m.s. value of a function f(x) with respect to x. The r.m.s. value in this case will be represented by $\{f\}_{(x)}$.

Note would be made here of an important difference between double arithmetic means and mixed r.m.s. - arithmetic means. Whereas

$$[f]_{(x,y)} = [[f]_{(x)}]_{(y)} = [[f]_{(y)}]_{(x)} = [f]_{(y,x)} \quad (7)$$

where f = f(x, y, . . .)

$$[\{f\}_{(x)}]_{(y)} \neq [\{f\}_{(y)}]_{(x)} \quad (8)$$

unless $<|f(x,y)|>$ is a square symmetric matrix (or of some other simpler but square form, which will not be discussed here), or, if non-square, if and only if all the matrix elements are of equal magnitude. Here it is implied by writing f(x, y, . . .) = f(x, y) that all other variables are held constant.

The values of $[\{\zeta_g\}_{(t)}]_{(\lambda)}$ and $[\{\zeta_g\}_{(\lambda)}]_{(t)}$ for Jan. 1970 are given in Table 2. It is seen that the two are quite comparable. Simple hand calculations show that the matrices $<|\zeta_g(\lambda, t)|>$ would yield the kind of values presented in Table 2 if the values of $|\zeta_g(\lambda, t)|$ are nearly equal or if standing eddies dominate the matrix. It will be seen below that the middle latitude vorticity field is dominated by (standing) wave number three. In the subtropics, fairly homogeneous values of $\zeta_g(\lambda, t)$ might be expected by climatological considerations. The reasons for the similarity

*NB: In this page f is not the Coriolis parameter.

Table 2

$[\{\zeta_g\}_{(\lambda)}]_{(t)}$ and $[\{\zeta_g\}_{(t)}]_{(\lambda)}$ for Jan. 1970.

Units: 10^{-7} s^{-1}

(For an explanation of symbols see Table 1)

$[\{\zeta_g\}_{(\lambda)}]_{(t)}$

Pressure	25 N	30 N	35 N	40 N	45 N	50 N	55 N	60 N	65 N	70 N	75 N
700 mb	185	179	198	223	243	245	235	249	237	236	254
500 mb	249	256	297	348	347	324	316	353	360	347	361
400 mb	295	330	367	437	414	383	370	413	412	394	398
300 mb	354	400	455	508	483	419	392	427	422	405	399
200 mb	373	419	508	490	412	318	286	302	293	284	268
100 mb	256	228	244	252	234	208	180	181	184	178	170

$[\{\zeta_g\}_{(t)}]_{(\lambda)}$

Pressure	25 N	30 N	35 N	40 N	45 N	50 N	55 N	60 N	65 N	70 N	75 N
700 mb	181	175	189	215	228	235	232	246	227	228	254
500 mb	246	255	291	334	335	320	318	349	345	336	357
400 mb	292	329	360	421	401	382	374	410	398	383	394
300 mb	350	399	450	495	468	420	394	423	408	392	390
200 mb	370	418	495	473	399	319	287	292	274	268	263
100 mb	249	226	236	238	216	193	172	173	171	167	167

of $[\{\zeta_g\}_{(t)}]_{(\lambda)}$ and $[\{\zeta_g\}_{(\lambda)}]_{(t)}$ at subpolar latitudes are not known at this time although characteristic periodicities of the eddies here might be suspected as causing the similarity.

The important conclusion from the above discussion is that the inequality (8) might be considered to be invalid for geostrophic relative vorticity in the extratropical winter troposphere. Hence

$$[\{\zeta_g\}_{(t)}]_{(\lambda)} \; \simeq \; [\{\zeta_g\}_{(\lambda)}]_{(t)} \; = \; K \tag{9}$$

5. The Distribution of Vorticity in Winter

Here we shall resume the discussion of Section 3.

Figure 8 illustrates $[\zeta_g]_{(\lambda, t)}$ which slightly indicates the tendency for the bifurcation of jet-stream level vorticity that we anticipated. We also note that 1) the subpolar zonal-and-time mean vorticity is not anticyclonic but cyclonic and 2) the arithmetic mean value of vorticity in the extratropics is generally much smaller (one-half or less) than the values of K in Table 2.

The reasons for observation 2) above are that although the vorticity associated with extratropical eddies is high, a fraction of it is transient, and this fraction is large in the subpolar latitudes as we shall see below. Time averaging eliminates this component. And when zonal averaging is performed additionally the standing eddies with their large magnitudes of vorticity are also eliminated. The remainder, which is the vorticity of the prevailing zonal mass (or geopotential height) distribution, is indeed very small.

The reasons for observation 1) are that the Arctic Front Jet (AFJ) tends to occur in conjunction with both ridges and troughs and therefore the relative geostrophic vorticity in the subpolar upper troposphere tends to fluctuate between large positive and negative values. The values of $[\zeta_g]_{(\lambda, t)}$ are the small differences between these large positive and negative values.

Figure 9 illustrates the distribution of the parameter K . As mentioned earlier the magnitude of K is everywhere much larger than that of $[\zeta_g]_{(\lambda, t)}$. Whereas $[\zeta_g]_{(\lambda, t)}$ distribution represents the vorticity of the prevailing latitudinal mass distribution only, K tends to conserve the components of vorticity associated with transient

and standing eddies, since the r.m.s. "averaging" neglects the differences in signs. In the neighborhood of the confluence of the Subtropical Jet Stream (STJ) and the Polar Front Jet Stream the ratio $[\zeta_g]_{(t,\lambda)}$:K reaches a maximum indicating the large zonal components of the winds in the STJ maxima and the relative large zonal wind shears north of these maxima (see Krishnamurti, 1961). The effect of these shears would appear in the $[\zeta_g]_{(t,\lambda)}$ distribution only if the waves in the STJ are of small amplitude. From the illustrations presented by Krishnamurti (op. cit.) and the distributions of $[\bar{u}]$ mentioned above this is seen to be true.

That the vorticity distribution represented by $[\zeta_g]_{(t,\lambda)}$ is the one associated with the mean mass distribution is apparent from Fig. 10, which is the January 1970 distribution of

$$([H]_{(t,\lambda)})_{(H)} = [H]_{(t,\lambda)} - [H]_{(t,\lambda,\phi)}$$

i.e., the deviation of zonal-mean geopotential height of isobaric surfaces from their hemispheric averages. By hemispheric mean we denote the average of $[H]_{(t,\lambda)}$ over the latitudes 20 N to 80 N. It is readily seen from this diagram that the windspeeds and shears associated with the mean mass distribution must result in the vorticity field of Fig. 8.

The components of vorticity associated with standing and transient eddies are very large away from the 200 mb, 35-42 N region, as seen in Fig. 9.

It might be considered that the 'normal' state of the extratropical troposphere is a disturbed state. Then the distribution of K might be said to represent the 'normal' state of the extratropical troposphere in winter for it conserves and presents the eddy effects (in addition to the influences of the time-and-longitude averaged mass field) unlike the $[\zeta_g]_{(t,\lambda)}$ distribution.

6. Vorticity Distribution and Tropopause Structure

A very distinguishing feature of the distribution of K is that the isopleths are quasi-horizontal whereas the isopleths of $[\zeta_g]_{(t,\lambda)}$ are nearly vertical everywhere. Moreover the vertical gradients of K are much larger above about 200-300 mb. Thus it is immediately apparent that a 'normal' distribution of this meteorological parameter, viz., vorticity, is capable of indicating a "lid" over tropospheric circulation features. The reason for this is that jet streams are wind systems associated with tropopause-breaks (see, for example, Reiter 1969C, p. 91-94.) The baroclinicity reversals associated with these breaks produce sharp reductions in vorticity above the jet-stream level (See proportionality 6 above.) The longterm zonal circulation vorticity, since it does not include all the meanders and temporal fluctuations of the jet streams, does not indicate these important reductions whereas the parameter K does.

We see from Fig. 9 that the Arctic Front Jet will normally occur at higher pressures than the Polar Front Jet and that the stratosphere is situated at higher levels in the tropics and midlatitudes than in the sub-polar regions.

7. The Geographical Distributions

In Fig. 11 the geographical distribution of $[\zeta_g]_{(t)}$ is given. Here the $0, \pm 100 \times 10^{-7}$ s $^{-1}$ contours have been omitted for clarity. Since the standing eddy component of vorticity has not been eliminated here as it is in the $[\zeta_g]_{(t,\lambda)}$ distribution the magnitudes of vorticity in the extratropics are higher.

Fig. 12 gives the geographical distribution of $\{\zeta_g\}_{(t)}$. This diagram is discussed below.

Middle Latitudes

A comparison of Fig. 11 and 12 shows that the midlatitude distribution of January mean vorticity has essentially a three-wave pattern, with maxima over the Atlantic and Pacific Oceans and over southern Asia. The magnitudes of $\{\zeta_g\}_{(t)}$ are larger than those of $[\zeta_g]_{(t)}$ everywhere. But the differences between $\{\zeta_g\}_{(t)}$ and $[\zeta_g]_{(t)}$ are not very large at the centers of the vorticity maxima. This shows that the three waves in the middle latitudes have a very large standing component.

All the three maxima are quasi-zonally distributed. The location of the maxima of $[\zeta]_{(t)}$ over the oceans is of particular significance. Both of these maxima have their major axes immediately over oceanic cold and warm current confluences (see, for example, Sverdrup, Johnson and Fleming, 1942, Charts II, IV and VII). The central contours of these maxima are located almost exactly over the east coasts of Asia and North America. The maxima do not protrude far into the continents.

Subpolar Latitudes

Here the values of $[\zeta_g]_{(t)}$ and $\{\zeta_g\}_{(t)}$ differ considerably in the regions of occurrence of vorticity extrema thus indicating the larger transient component of vorticity in these latitudes, compared to midlatitudes.

Perhaps the most interesting feature of these illustrations meteorologically is that the baroclinic field of the extratropical troposphere is divided into two extrema. The vorticity field associated with the midlatitude maxima are located over regions of maximum ocean surface temperature contrast. The vorticity maxima are also located over regions (especially off the East Coast of the USA) where the prevailing winds have significant southerly components. Thus if the vorticity advection theory of development (Reiter 1963, p. 326-332) is applied in these regions, an extremely large amount of kinetic energy would be seen generated by the nascent extratropical cyclones over the regions of ocean current confluence. This generation must overcompensate frictional dissipation and appear in the subpolar latitudes as the Arctic Front Jet. Although the above statements are purely qualitative the author feels that the midlatitude distribution of vorticity maxima significantly influences the region of occurrence of the AFJ. It is possible that the vorticity patterns associated with the AFJ similarly affect the kinetic energy distribution in the middle latitudes but much more intermittently since the AFJ indeed is more transient than the PFJ as might be seen from daily geopotential height fields of the 300 mb surface. The greater part of the kinetic energy of the PFJ is probably derived from interaction with the STJ. These regions have been established by Krishnamurti (1961) to be the regions where the vorticity maxima occur in midlatitudes.

Krishnamurti (1961) showed that in the meridional sectors where the subtropical highs protrude poleward, the troughs associated with the PFJ plunge equatorward. This is also brought out in Fig. 11. But there seems to be very little interaction of this type over southern Asia. This is also true of another analysis performed by the author. Fig. 13 gives the zonal distribution of $\{\zeta_g\}_{(t)}$ at 300 mb, 60 N and of $[\zeta_g]_{(t)}$ at 200 mb, 25 N. From this diagram it is seen that the most barotropic (i.e., smallest values of $\{\zeta_g\}_{(t)}$ regions in the subpolar latitudes are located in the meridional sectors where the subtropical highs protrude farthest poleward; these are also the sectors where the vorticity is a maximum in the midlatitudes.

In view of the observed barotropy in the subpolar latitudes in these meridional sectors, the baroclinic regions in the subpolar latitudes must be in the meridional sectors between those in which the midlatitude distribution of baroclinicity has maxima. This is seen to be the case from Fig. 12. The exception to this rule again occurs over Asia where the midlatitude and subpolar maxima of $\{\zeta_g\}_{(t)}$ occur in the same meridional sector.

8.   Some Anomalies of the Circulation of January 1970

An excellent analysis of the circulation of Jan. 1970 has been presented

by Wagner (1970). He notes a number of anomalies of the January 1970

circulation. We consider two of these as of particular significance.

Wagner (op. cit.) notes that "the broad cyclonic flow over the oceans at

midlatitudes was associated with anomaly centers of 100 and 170 m below

normal over the Pacific and Atlantic respectively" at the 700 mb level.

The anomalies at the 300 mb level were not given. But if conditions similar

to those at the 700 mb level were prevalent there, we should expect that the

vorticity extrema over the two oceans are normally less well developed than

indicated by Fig. 8 and 9.

Wagner (op. cit.) also presents the departures from normal of average

surface temperature for January 1970 for the U. S. These are mostly positive west of

105 W and negative east of that longitude. If these could be thought of as

being brought about by upper tropospheric troughs, then, normally the vorticity

maxima over the oceans must protrude more into the continents than indicated

by Fig. 8 and 9.

9. Conclusions

From our results we conclude that the upper tropospheric vorticity field and the tropospheric-mean baroclinic field of the extratropical troposphere are bifurcated in winter. The extrema of vorticity occur over 30-45 N and 60-70 N with a relative minimum at 55 N.

A parameter such as time-averaged zonal root mean square vorticity is capable of bringing out this feature in time-and-zonal average distributions

If these distributions have pressure as vertical coordinate, the existence of a stratosphere which appears as a lid over tropospheric circulation features could be obtained.

These distributions indicate clearly the normal location of the frontal jet streams of the extratropical troposphere which are otherwise lost in averaging.

Acknowledgements

Bibliography

Krishnamurti, T. N., 1961. The subtropical jet stream of winter, J. Meteorol., 18:172-191.

Kung, Ernest C., 1971. A diagnosis of adiabatic production and destruction of kinetic energy by the meridional and zonal motions of the atmosphere, Quart. J. Royal Met. Soc., 97:61-74.

Lorenz, Edward N., 1967. The nature and theory of the general circulation of the atmosphere, World Meteorological Organization, No. 218. TP. 115, 161 pp.

Oort, Abraham H., 1964. On estimates of the atmospheric energy cycle, Mon. Weather Rev., 92:483-493.

Oort, Abraham H., and Rasmusson, Eugene M., 1971. Atmospheric circulation statistics, NOAA Professional Paper 5, (U.S. Govt. Printing Office, Washington, D.C. Stock Number 0317-0045) 323 pp.

Petterssen, Sverre, 1956. Weather analysis and forecasting, Vol. 1. McGraw Hill Book Co. Inc., 428 pp.

Reiter, Elmar R., 1963. Jet-Stream Meteorology. Univ. of Chicago Press, Chicago, Ill. 515 pp.

Reiter, Elmar R., 1969a. Mean and eddy motions in the atmosphere. Mon. Wea. Rev., 97:200-204.

Reiter, Elmar R., 1969b. Atmospheric Transport Processes, Part 1: Energy Transfers and Transformations. TID-24868, U.S. Atomic Energy Commission, Division of Technical Information Extension, Oak Ridge, Tenn. 212 pp.

Reiter, Elmar R., 1969c. Tropospheric Circulation and Jet Streams, in World Survey of Climatology, Vol. 4: Climate of the Free Atmosphere (D. F. Rex, Ed.), Elsenier Publishing Co., Amsterdam-London-New York 1969. 85-202.

Reiter, Elmar R., 1972. Atmospheric Transport Processes, Part 3: Hydrodynamic Tracers. TID-25731, U.S. Atomic Energy Commission, Division of Technical Information Extension, Oak Ridge, Tenn. 212 pp.

Sverdrup, Harold Ulrik, Johnson, Martin W., and Fleming, Richard H., 1942. The Oceans, Prentice-Hall Inc., Englewood Cliffs, N.J. 1087 pp.

Wagner, James A., 1970. The weather and circulation of January 1970: Record cold in the eastern third of the nation and record rainfall in the Pacific Northwest. Mon. Wea. Rev., 98:328-334.
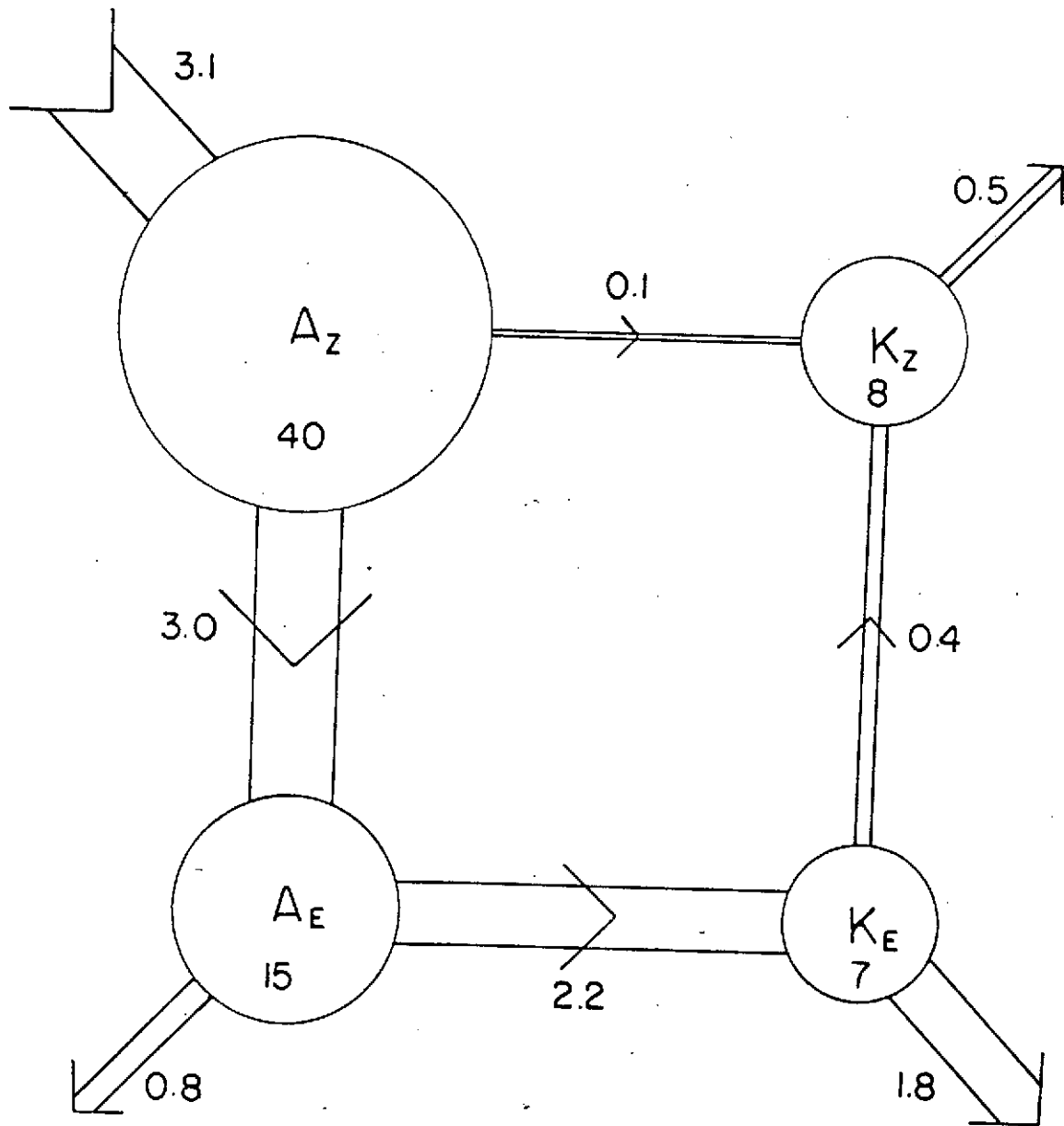
Fig. 1. The energy cycle of the atmosphere as estimated by Oort (1964). Values of energy are in units of 10^5 joules m^{-2}, and values of generation, conversion and dissipation are in watts m^{-2}.
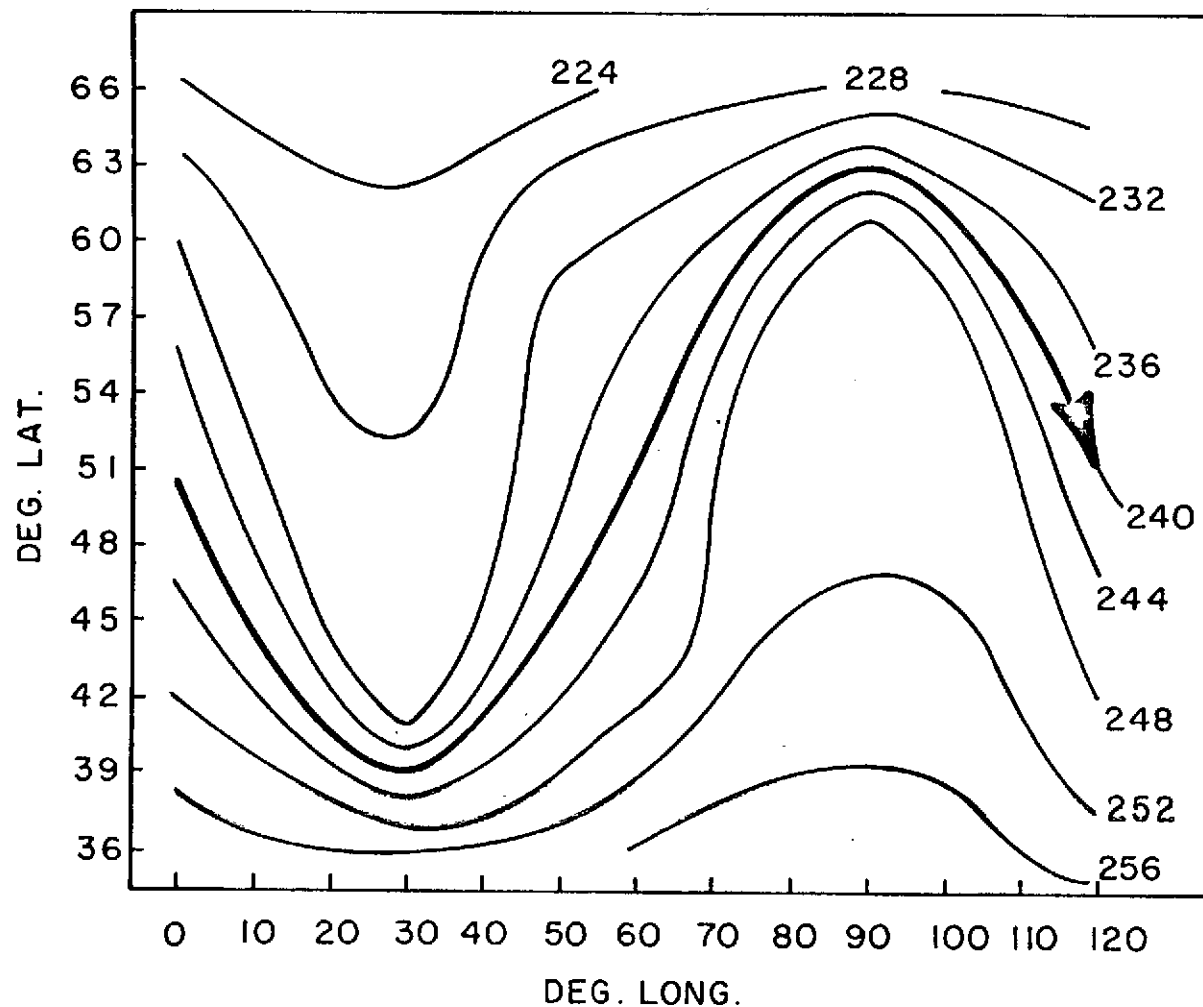
Fig. 2. Schematic illustration of jet-stream level flow and the distribution of underlying layer-mean temperature. The jet axis, the heavy line with arrow-head, is a line joining the maximum wind speeds. The surface wind speed is assumed to be zero everywhere. Hence jet-stream level streamlines are parallel to the layer-mean isotherms (^{O}K).
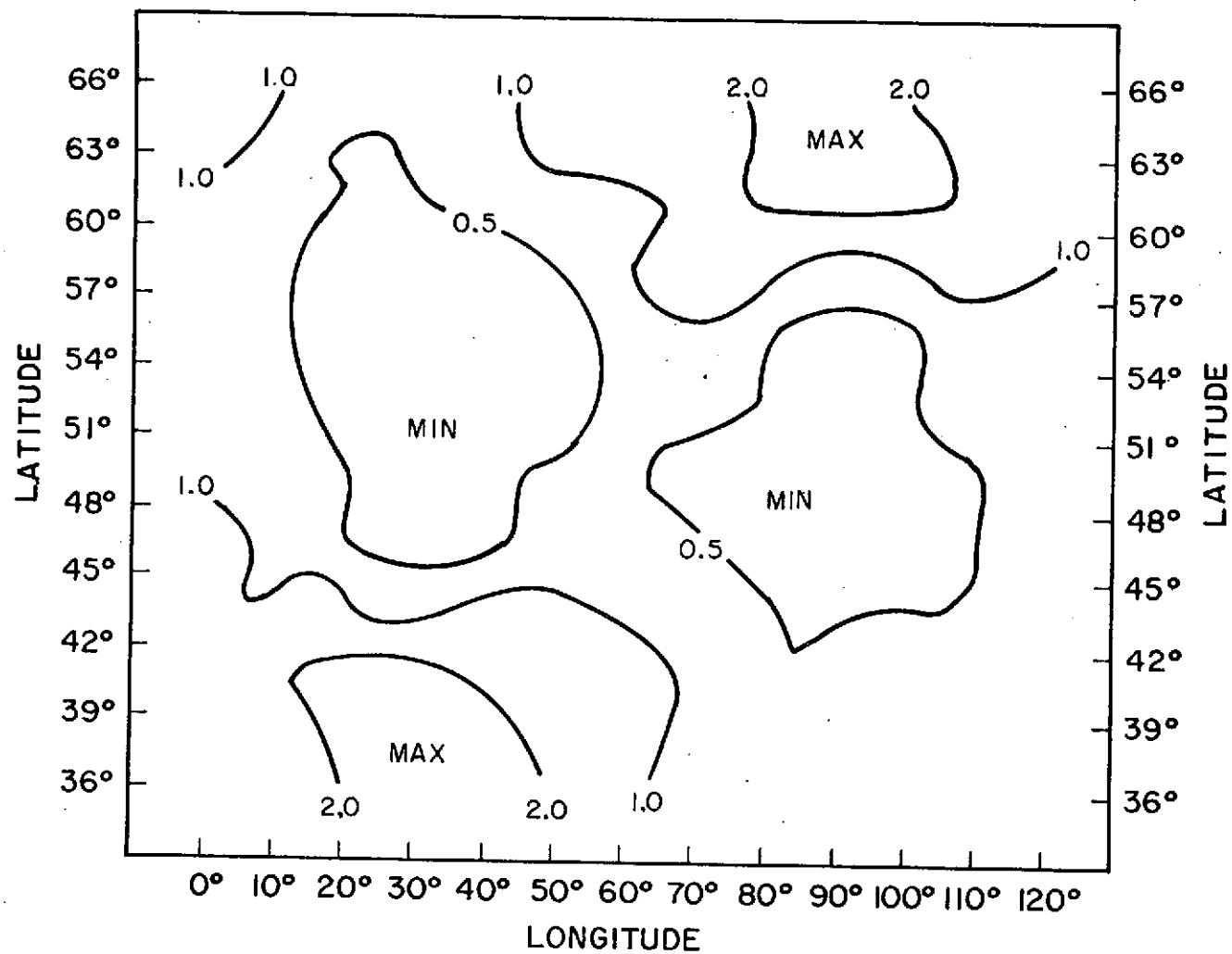
Fig. 3. The meridional temperature gradients $\partial\overline{T}/\partial y$ corresponding to Fig. 2. Units are $^{\circ}K \ (100 \ Km)^{-1}$.
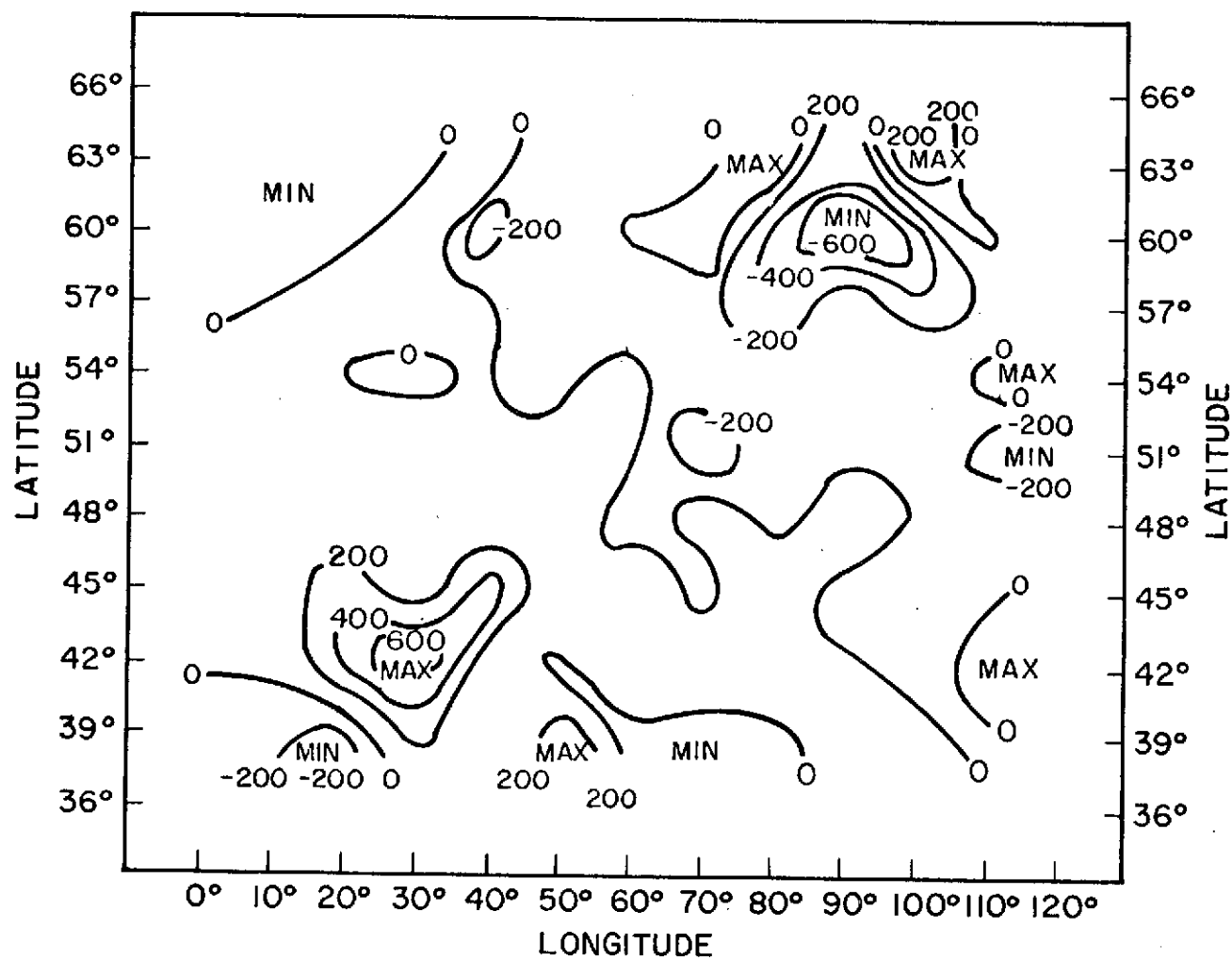
Fig. 4. The distribution of $\nabla_2^2 \overline{T}$ corresponding to Fig. 2. Units are $K/10^7 Km^2$.
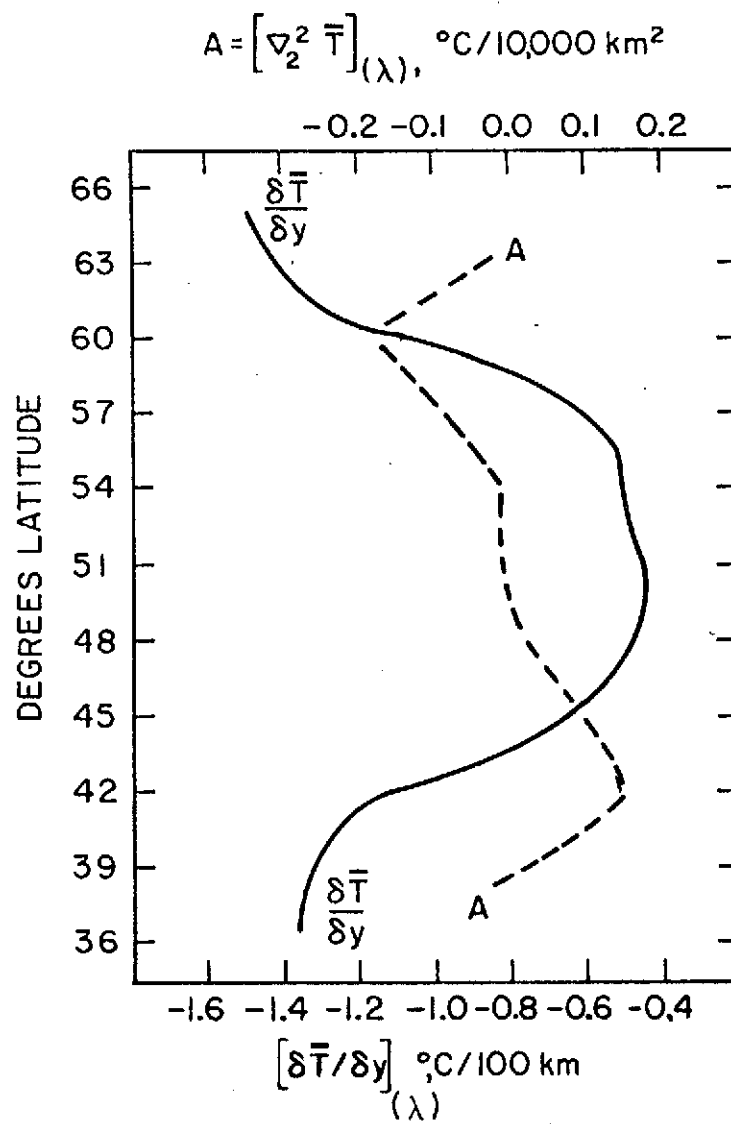
Fig. 5. The zonal averages of $\partial \bar{T}/\partial y$ and $\nabla_2^2 \bar{T}$ for the model of Fig. 2.
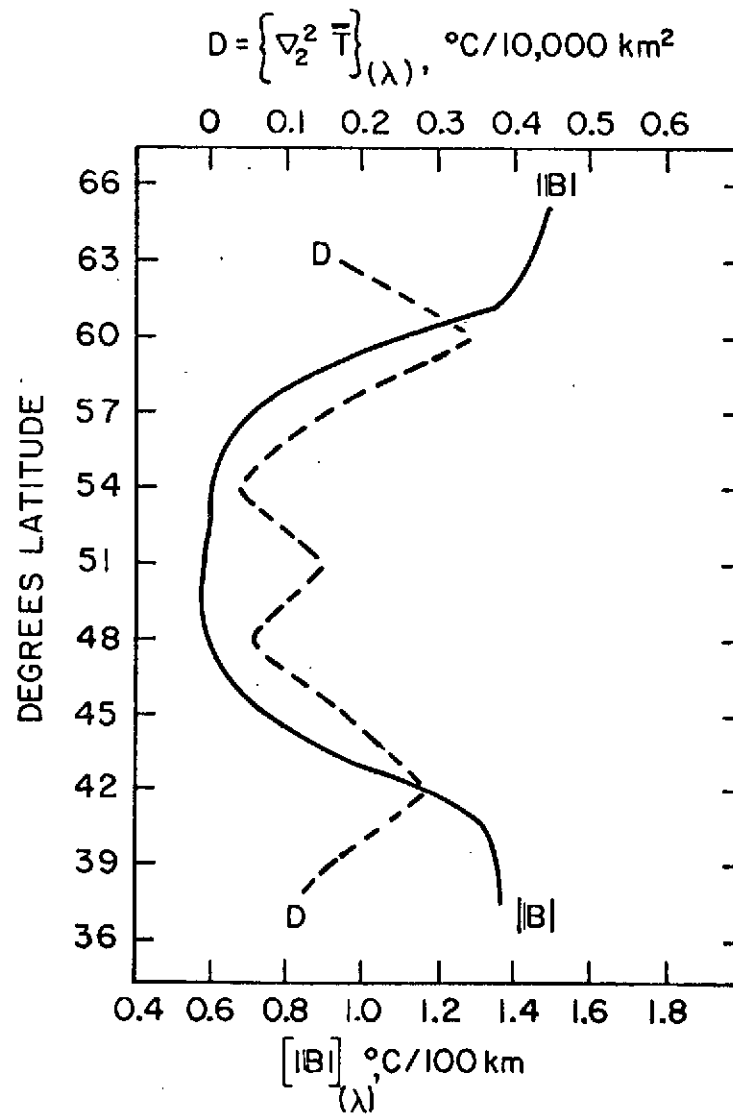
Fig. 6. The zonal averages of the magnitude of the baroclinicity vector
$|\mathcal{B}|$; and the zonal r.m.s. values of $\nabla_2^2\bar{T}$ for the model of Fig. 2.
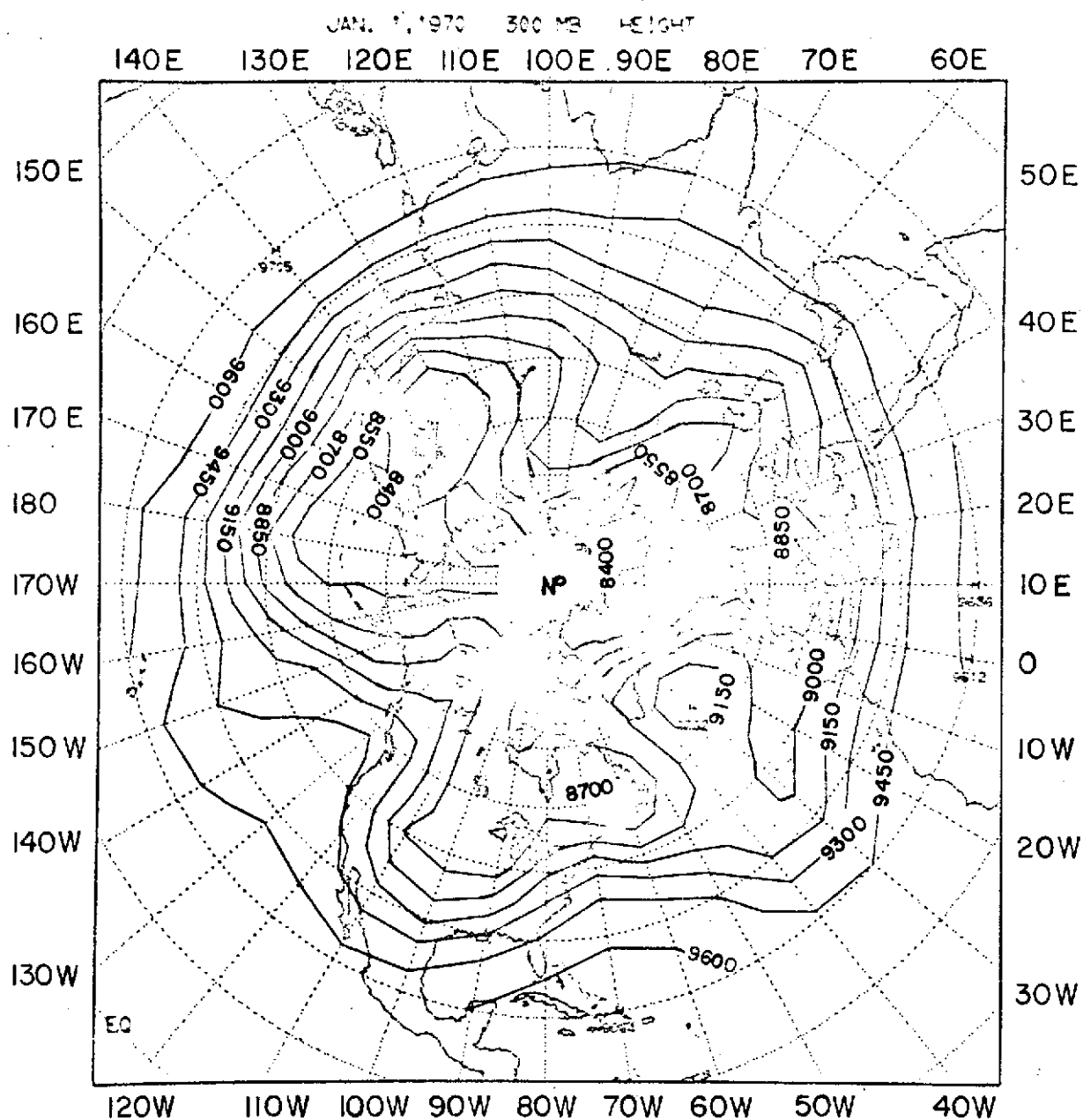
Fig. 7. The geopotential height distribution of the 300 mb surface for Jan. 1, 1970. Units: geopotential meters.
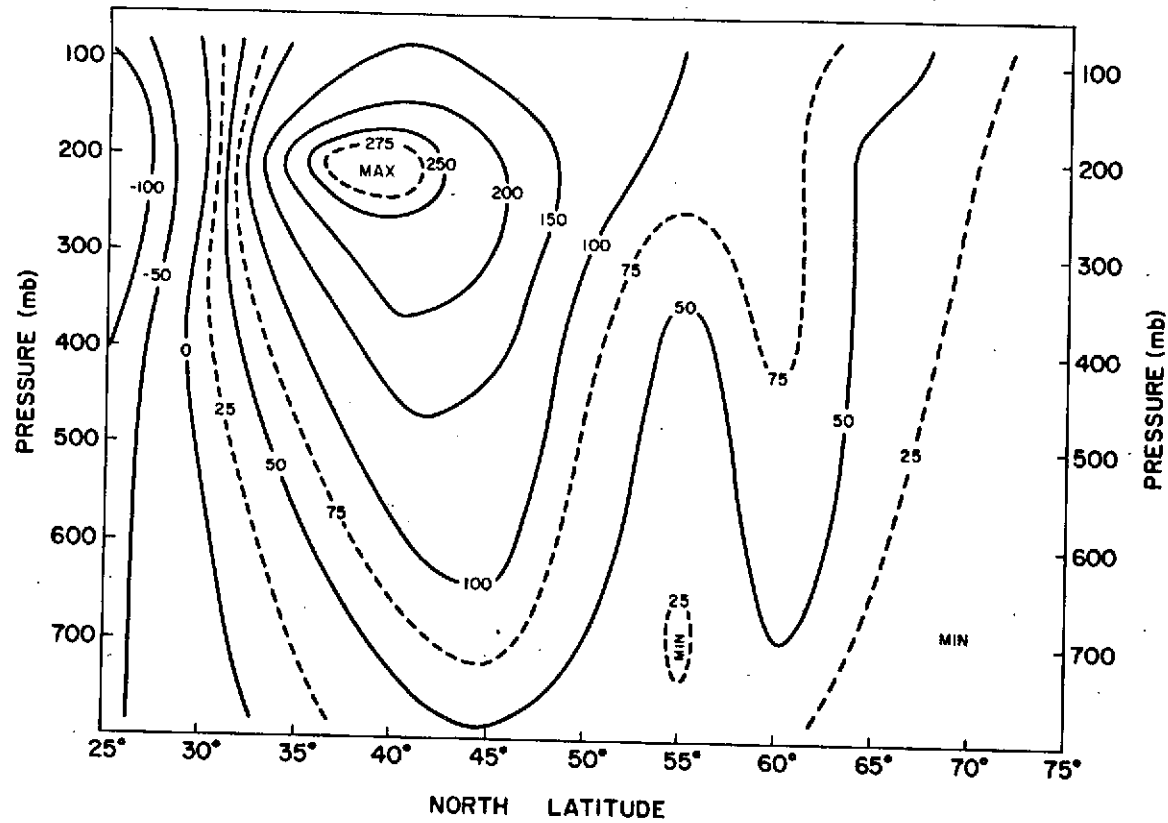
Fig. 8. The distribution of $[\zeta_g]_{(\lambda,t)}$ for Jan. 1970. Units: $10^{-7}s^{-1}$. Symbolism defined in Table 1.
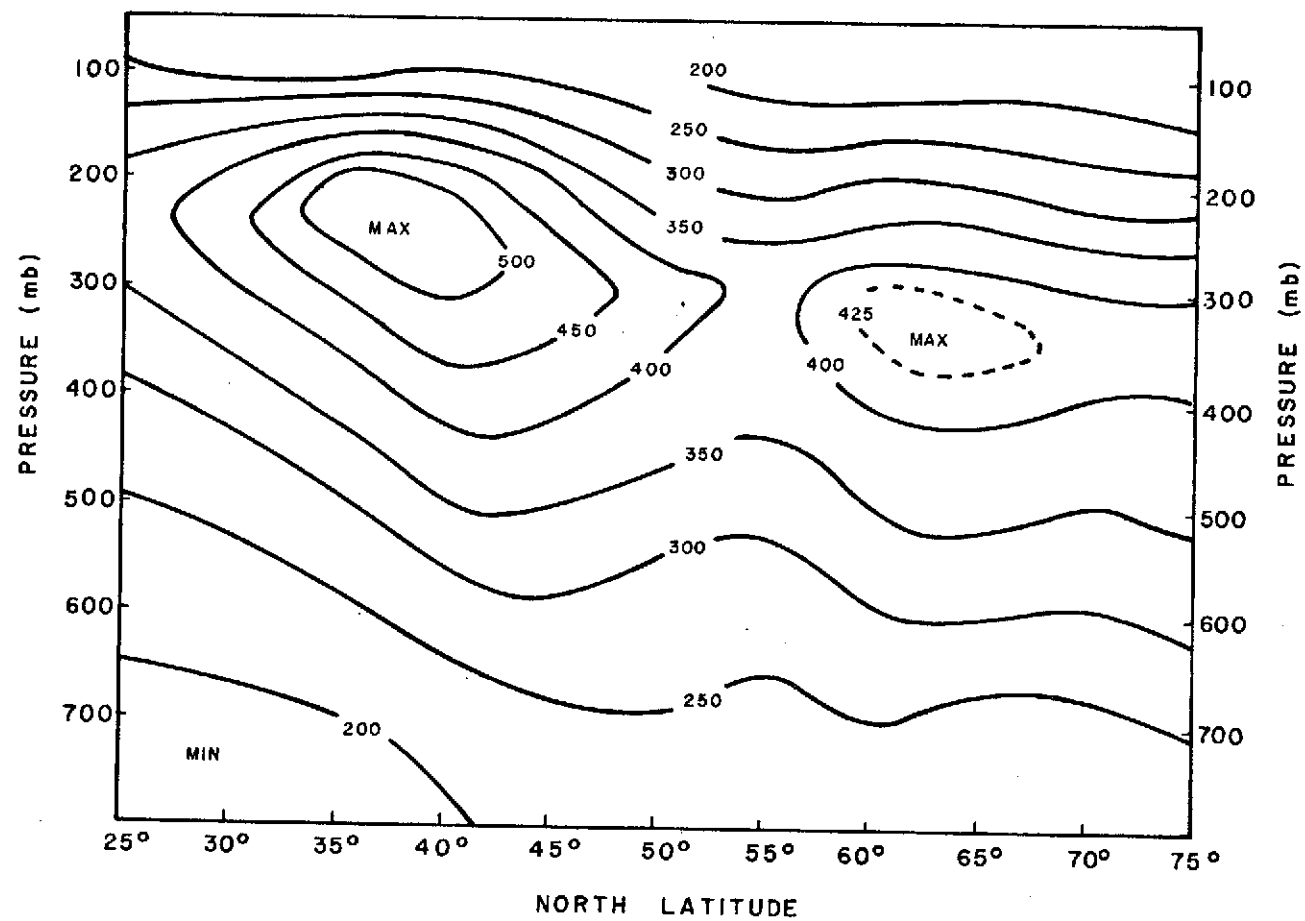
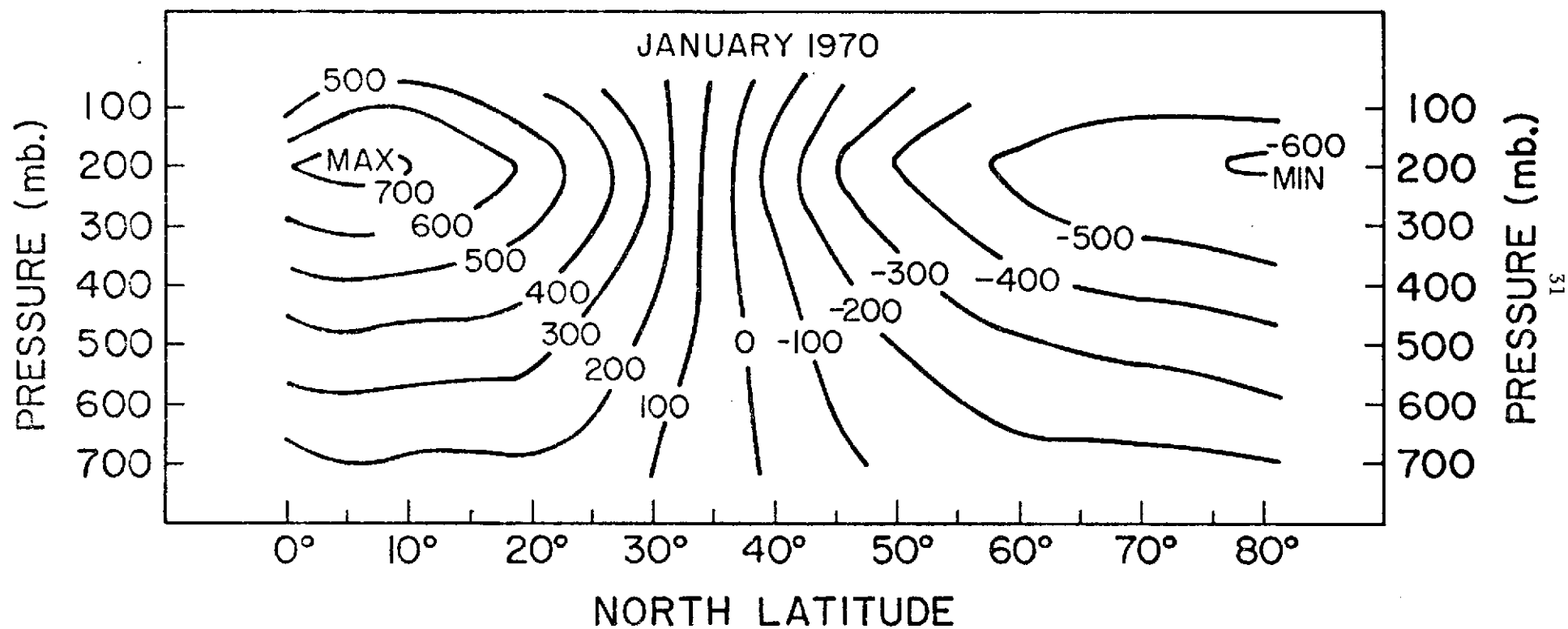Fig. 9. The distribution of K for Jan. 1970. Units: $10^{-7}s^{-1}$. Symbols defined in Table 1.

Fig. 10. The distribution of $([H]_{(t,\lambda)})_{(\phi)}$ in Jan. 1970. Units: Geopotential meters. For an explanation of symbols see Table 1.
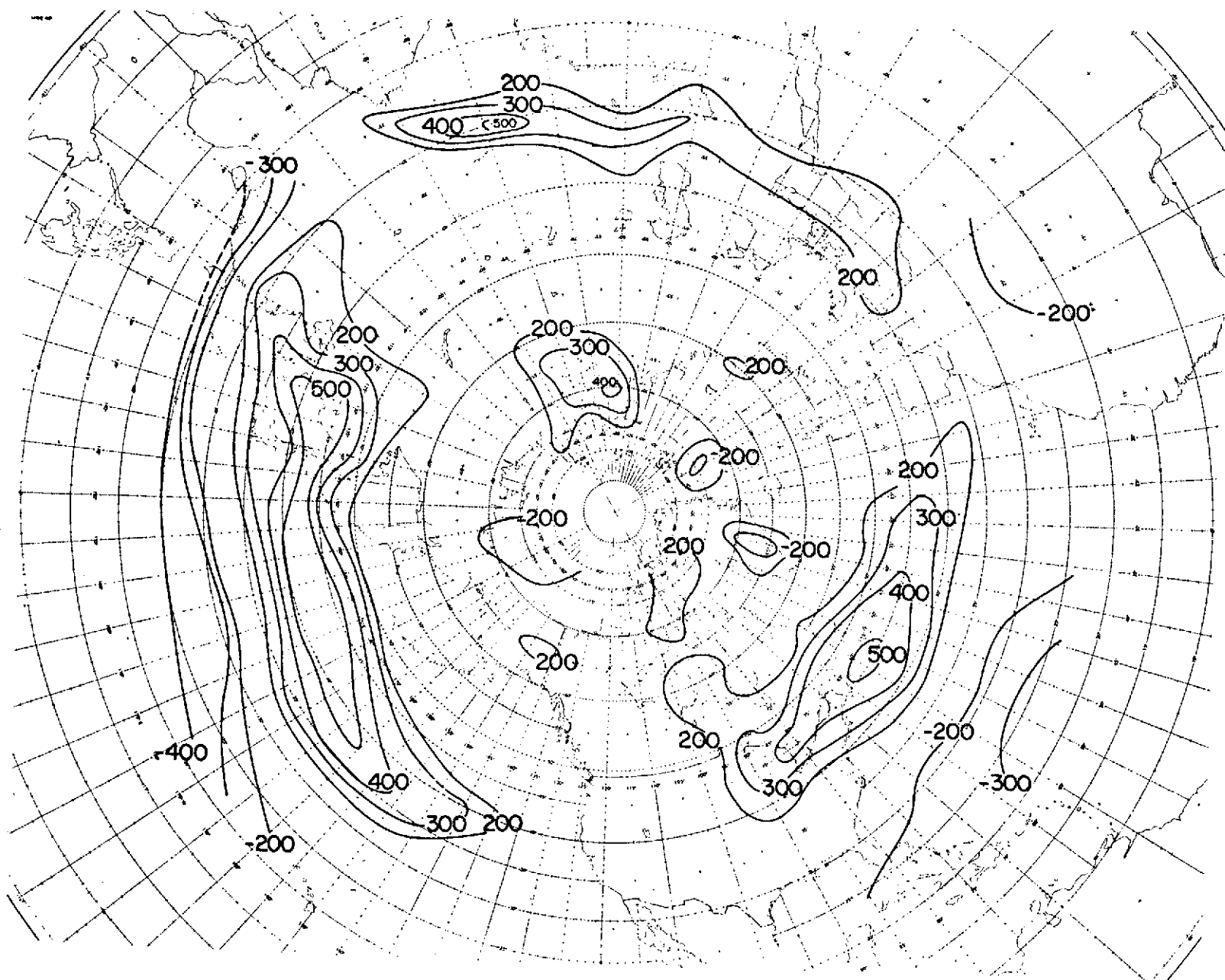
Fig. 11. The geographical distribution of $[\zeta_g]_{(t)}$ at 300 mb in Jan. 1970. Units: $10^{-7} s^{-1}$. The 0, 100, -100 contours were omitted for the sake of clarity.
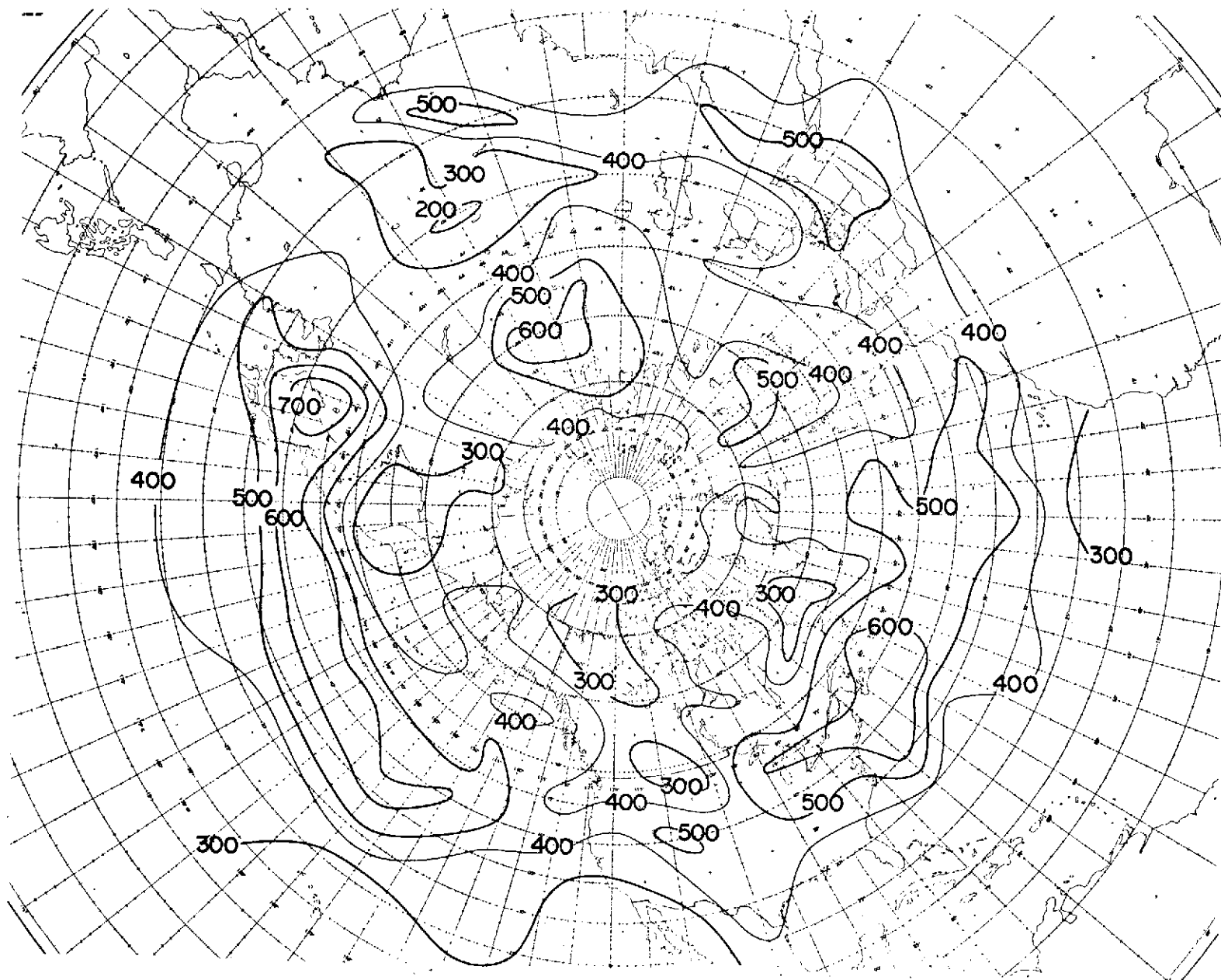
Fig. 12. The geographical distribution of $\{\zeta_g\}_{(t)}$ at 300 mb in Jan. 1970.
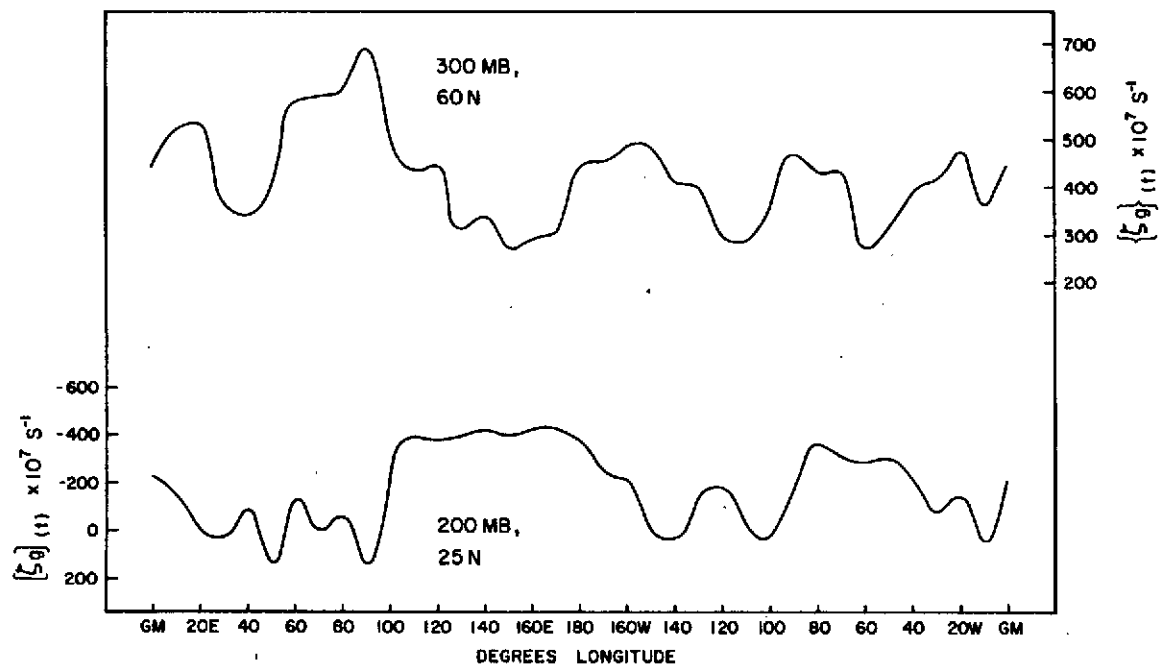Units: $10^{-7} s^{-1}$.

Fig. 13. The zonal distribution of $\{\zeta_g\}_{(t)}$ at 300 mb at 60 N and of $[\zeta_g]_{(t)}$ at 200 mb at 25 N in Jan. 1970.